CHAPTER I

INTRODUCTION

Background and signification of the research problem

Diabetes Mellitus (DM) is one of the most common chronic diseases with estimated 387 million patients worldwide and responsible for 4.9 million deaths in 2014 (1). Global Report on Diabetes released by World Health Organization (WHO) in 2016, DM has affected more than 422 million adults globally and the number is expected to rise beyond 592 million in 2035 (2). Diabetes is a group of metabolic diseases characterized by high blood glucose levels. Untreated chronic hyperglycemia could block or even damage the body's blood vessels, eventually leading to severe complications such as heart attack, stroke, kidney failure, leg amputation, vision loss and nerve damage. People living with type 2 DM are more vulnerable to various forms of both short- and long-term complications, which often lead to premature death. This tendency of increased morbidity and mortality is seen in patients with type 2 DM because of the commonness of this type of DM, its insidious onset and late recognition, especially in resource-poor developing countries like Africa (3). One of the important therapeutic approaches is to inhibit digesting enzymes such as α-glucosidase or α-amylase in the intestine to slow down the digestion and absorption of sugar and to suppress post-prandial hyperglycemia. Recently, α-glucosidase has been recognized as a therapeutic target for treating type-2 DM based on its pivotal role in the digestion of carbohydrates. Several α-glucosidase inhibitors such as acarbose, miglitol and voglibose have been widely used in treating type-2 DM. However, various side effects including bloating, flatulence and diarrhea are encountered throughout the treatments (4). Because of this, new and safer α-glucosidase inhibitors with minimal side effects are urgently warranted. Flavonoid compounds, the natural phenyl-substituted chromones, i.e., luteolin and naringenin, have been reported to act as potential glucosidase inhibitors that provide protective effects in diabetes therapy both *in vitro* and *in vivo* (5).

α-Glucosidase inhibitors can be used as a first-line drug in newly diagnosed type 2 diabetes insufficiently treated with diet and exercise alone, as well as in combination with all oral antidiabetics and insulin if monotherapy with these drugs fails to achieve the targets for HbA1c and post-prandial blood glucose (6). α-Glucosidase inhibitors, such as acarbose, miglitol and voglibose, which are carbohydrate mimetics or derivatives, have already been marketed for the treatment of type II diabetes mellitus. These drug molecules can decrease postprandial hyperglycemia and hyperinsulinemia, introducing gastrointestinal adverse effects including diarrhea, flatulence and abdominal discomfort. Developing more efficient and safer inhibitors for hyperglycemia control in diabetes remains a global health priority. Flavonoid compounds such as luteolin, and naringenin, also have been reported to act as potential glucosidase inhibitors that provide protective effects in diabetes therapy both *in vitro* and *in vivo* (5). Moreover, Yeast α-glucosidase is potently inhibited by the anthocyanidin, isoflavone, and flavonol groups with IC_{50} values less than 15 μM. Rat's small intestinal α-glucosidase is weakly inhibited by many flavonoids and slightly by the anthocyanidin and isoflavone groups (7).

Several phenyl-substituted chromones, also called flavonoids, have been reported to possess a wide variety of biological activities, i.e., anti-HIV, anticancer, antimicrobial, antioxidant, anti-inflammatory and anti-parasitic activities (8-10). In our previous studies, we have reported the anti-HIV-1 protease (11), antioxidant (12), antimalarial (13), anti-topoisomerase I (14) and anti-inflammatory (15) activities of a series of chromone compounds. Therefore, chromone compounds are expected to act as potential α-glucosidase inhibitors in this study.

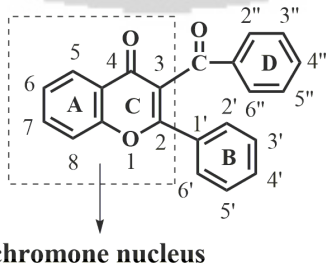

Figure 1.1 General structure of flavonoids.

Objectives

1. To evaluate the inhibitory activity of the chromone compounds against α-glucosidase.

2. To study the binding interaction between the chromone compounds against α-glucosidase.

Hypothesis

1. The designed chromone compounds possess potent α-glucosidase inhibitory activity.

2. The designed chromone compounds have the potential to bind with α-glucosidase.

Scope of the research

Biological activity testing and molecular docking study of chromone compounds as α-glucosidase inhibitors.

Expected benefits

This research aims to evaluate the inhibitory activities of chromone derivatives against α-glucosidase and study the binding interaction between the chromone compounds and α-glucosidase. The results will lead to the development of novel diabetes agents targeted at α-glucosidase.

CHAPTER II

LITERATURE REVIEW

DM is a prevalent metabolic disorder characterized by prolonged fasting hyperglycemia resulting from inadequate production (type 1) or inefficient utilization of insulin (type 2). Type 2 DM (formerly known as non-insulin dependent DM) is the most common form of DM, characterized by hyperglycemia, insulin resistance, and relative insulin deficiency. Insulin resistance is the main abnormality in type 2 DM (16). Development of the insulin radioimmunoassay leads to the finding that patients with early-maturity-onset diabetes produce insulin and secrete this hormone in response to nutrient ingestion. Subsequently, defects in the ability of islet β cells to respond to intravenous secretagogues (including glucose) have been reported in these patients (17). Additionally, these patients did not respond well to insulin and were thus deemed to be insulin insensitive. This insulin insensitivity contributed to increased glucose production by the liver and decreased glucose uptake in muscle and adipose tissue (18). Nowadays, some of these abnormalities are attributed to adiposity, especially adiposity within the intra-abdominal cavity. Prolonged high blood glucose levels in diabetes patients can lead to severe diseases that affect the heart, blood vessels, eyes, kidneys, and nerves.

2.1 Recent antidiabetic drugs

1. Biguanides

Biguanides such as metformin are the most commonly used in overweight and obese patients, suppress hepatic glucose production, increase insulin sensitivity, enhance glucose uptake, increase fatty acid oxidation, and decrease glucose absorption from the gastrointestinal tract. Due to the development of lactic acidosis, metformin should be used cautiously in elderly diabetic individuals with renal impairment (19).

2. Sulfonylureas

Sulfonylureas stimulate endogenous insulin secretion; therefore, the drugs in this group carry a risk of hypoglycemia. Elderly patients with DM treated with sulfonylureas have a 36% increased risk of hypoglycemia compared to younger patients. Glyburide is associated with higher rates of hypoglycemia compared to glipizide. Some risk factors for hypoglycemia are age-related impaired renal function, simultaneous use of insulin or insulin sensitizers, age greater than 60 years, recent hospital discharge, alcohol abuse, caloric restriction, multiple medications or medications that potentiate sulfonylurea actions (20).

3. Meglitinides

Repaglinide and Nateglinide are non-sulfonylurea secretagogues that act by stimulating the release of insulin from the beta cells, similar to sulfonylurea. Meglitinides have a rapid onset and a short duration of action (4-6 hours) and thus lower the risk of hypoglycemia. Meglitinides are given before meals for postprandial blood glucose control. Pre-prandial administration allows flexibility in case a meal is missed without increased risk of hypoglycemia. Repaglinide is mainly metabolized in the liver with minimal amounts excreted by the kidneys. Thus dose adjustment is unnecessary in patients with renal insufficiency except for those with end-stage renal disease (21, 22).

4. Thiazolidinediones

Thiazolidinedione is an insulin sensitizer. They are the first drugs to prevent the basic problem of insulin resistance in type 2 DM patients, whose class now includes mainly pioglitazone after the restricted use of rosiglitazone recommended by the Food and Drug Administration (FDA) recently due to increased cardiovascular events reported with rosiglitazone. Pioglitazone use is not associated with hypoglycemia and can be used in cases of renal impairment and is thus well tolerated in older adults. On the other hand, due to concerns regarding peripheral edema, fluid retention and fracture risk in women, its use can be limited in older adults with DM. Pioglitazone should be avoided in elderly patients with congestive heart failure and is contraindicated in patients with class III-IV heart failure (23, 24).

5. α-Glucosidase inhibitors

Acarbose, Voglibose and Miglitol are α-glucosidase inhibitors. These agents are most effective for postprandial hyperglycemia and should be avoided in patients with significant renal impairment. Their use is usually limited due to high rates of side effects such as diarrhea and flatulence. Voglibose has been shown to significantly improve glucose tolerance (25, 26).

6. Incretin-based therapies

Glucagon-like peptide 1 (GLP-1) analogues d body weight control. They are available for use as monotherapy, as an adjunct to diet and exercise or in combination with oral hypoglycemic agents in adults with type 2 DM. Examples are exenatide, an incretin mimetic, and liraglutide (25, 27).

7. Dipeptidyl-peptidase IV inhibitors

Dipeptidyl-peptidase IV (DPP-IV) inhibitors inhibit DPP-IV. This ubiquitous enzyme rapidly inactivates GLP-1 and gastric inhibitory polypeptide (GIP), increases active levels of these hormones and improves islet function and glycemic control in type 2 DM. DPP-IV inhibitors are a new class of anti-diabetes drugs that provide comparable efficacy to current treatments. They are effective as monotherapy in patients inadequately controlled with diet and exercise and as add-on therapy in combination with metformin, thiazolidinediones, and insulin (28,29).

8. Insulin

Insulin is used alone or in combination with oral hypoglycemic agents. Augmentation therapy with basal insulin is useful if some β cell function remains. Replacement of basal-bolus insulin is necessary if β cell exhaustion occurs. Rescue therapy using replacement is necessary in cases of glucose toxicity which should mimic the normal release of insulin by the beta cells of the pancreas (30).

9. Insulin analogues

Insulin therapy is limited in its ability to mimic normal physiologic insulin secretion. Traditional intermediate- and long-acting insulins are limited by inconsistent absorption and peaks of action that may result in hypoglycemia. The pharmacokinetic profiles of the new insulin analogues are distinct from those of the regular insulins, and their onset and durations of action range from rapid to

prolonged. Currently, two rapid-acting insulin analogues, insulin lispro and insulin aspart, and one long-acting insulin analogue, insulin glargine, are available (31, 32).

10. SGLT2 inhibitors

SGLT2 inhibitors are an excellent choice for type 2 DM treatment where blood glucose levels are lowered without hampering insulin secretion (33, 34). In healthy adults, approximately 180 L of plasma containing 5.5 mM glucose is filtered through the kidney. Around 180 g of glucose is filtered through the glomeruli and lost primarily through urine. SGLT2 is 1 of the 12 components of the SLC5A, affixed to the S1 segment of the proximal convoluted tubule in the kidney, and it accounts for the extensive (>90%) filtration of glucose via glomeruli of the kidney (33-37). The uptake of remnant glucose is managed by the second member of the solute carrier family SGLT1, which is predominantly expressed in the S2/S3 segments of the proximal-convoluted tubule and parts of the small intestine. Once the glucose is reabsorbed from the kidneys, it is transferred to the circulatory system, posing a potential risk for diabetic patients. The action of SGLT2 inhibitors is focused on the inhibition of these receptors leading to moderate levels of glucose. This glucose is excreted in the urine, thereby maintaining the optimum blood glucose levels in the body (33, 38, 39). SGLT2 inhibitors are the most well-tolerated class with no major adverse effects and are considered advantageous in various circumstances.

Phlorizin was the earliest SGLT2 inhibitor discovered. It is a naturally occurring O-glycoside found throughout many plants and the barks of apple trees that are commonly known to produce glycosuria (33, 40). Even though phlorizin can reduce elevated blood glucose levels in animals, it cannot be used as a hypoglycemic agent due to various concerns. Phlorizin has an IC_{50} value of 34.6 nM for hSGLT1 and 210 nM for hSGLT2, respectively (33, 41). The first concern is that phlorizin acts as a nonselective SGLT2 inhibitor. It would also inhibit SGLT1 and lead to GI side effects such as diarrhea and dehydration (33, 42-44). Furthermore, phlorizin, an O-glucoside, is quickly metabolized in the intestinal tract by β-glucosidase upon oral administration (33, 45). To overcome these problems, various drugs derived from phlorizin were further developed and marketed, including

dapagliflozin, canagliflozin, ipragliflozin, empagliflozin, luseogliflozin, tofogliflozin, sotagliflozin, ertugliflozin and bexagilflozin (33, 41).

2.2 α-Glucosidase enzyme

Glucosidases are named based on their substrates, types of linkages hydrolyzed, and precise mechanism of action. α-Amylases (i.e., salivary and pancreatic α-amylases) act on long-chain carbohydrates, while α-glucosidases (i.e., maltase-glucoamylase and sucrase-isomaltase) hydrolyzes carbohydrates by acting on the 1,4-α linkages, thereby releasing α-d-glucose from the non-reducing end of the sugar (Figure 2.1). The end product of starch digestion by α-glucosidases such as Glucoamylase (MGAM) is glucose. The released glucose will then be absorbed into the bloodstream resulting in increased blood glucose level (46). Consequently, postprandial blood glucose level becomes under control and helps to cure type II DM. Recently, α-glucosidase has been recognized as a therapeutic target for treating type-2 DM based. The reductions in HbA_{1c} observed with the α-glucosidase inhibitors are in the range observed with other medication classes (47).

There are two main classes of carbohydrate digesting enzymes that are:

1. α-Amylases:

1.1) Salivary α-amylase starts acting in the mouth, cleaving endo α-(1,4) linkages in starch molecules to generate shorter oligomers.

1.2) Pancreatic α-amylase (HPA) acts on the products of salivary α-amylase digestion in the gut to further hydrolyze endo α-(1,4) glycosidic linkages and yield much smaller oligosaccharides like maltose (disaccharide), maltotriose (trisaccharide), and α-limit dextrin (a mixture of polymers of D-glucose units linked by α-(1,4) and α-(1,6) glycosidic bonds).

2. α-Glucosidases:

Products of amylase hydrolysis cannot be absorbed by the intestine, so they are further broken down into simpler sugars or monosaccharides (e.g., glucose, galactose, and fructose) by small membrane-bound intestinal enzymes, such as

2.1) Maltase-glucoamylase (MGAM) cleaves the non-reducing α-(1,4) glycosidic linkages to release α-D-glucose.

2.2) Sucrase-isomaltase (SI) can also cleave α-(1,4) glycosidic linkages to release α-D-glucose. In addition, the N-terminal domain of sucrase-isomaltase (NtSI) cleaves the α-(1,6) linkage of amylopectin, while the C-terminal domain of sucrase-isomaltase (CtSI) can cleave the α-(1,2) linkage of sucrose.

Structures of both α-amylases and α-glucosidases are characterized by a barrel composed of 8 β strands and α helices. While the former class of enzyme has both Asp and Glu residues in the active site and belongs to the glycoside hydrolase family 13 (GH13), the latter has only Asp residues in the active site and belongs to the glycoside hydrolase family 31 (GH31).

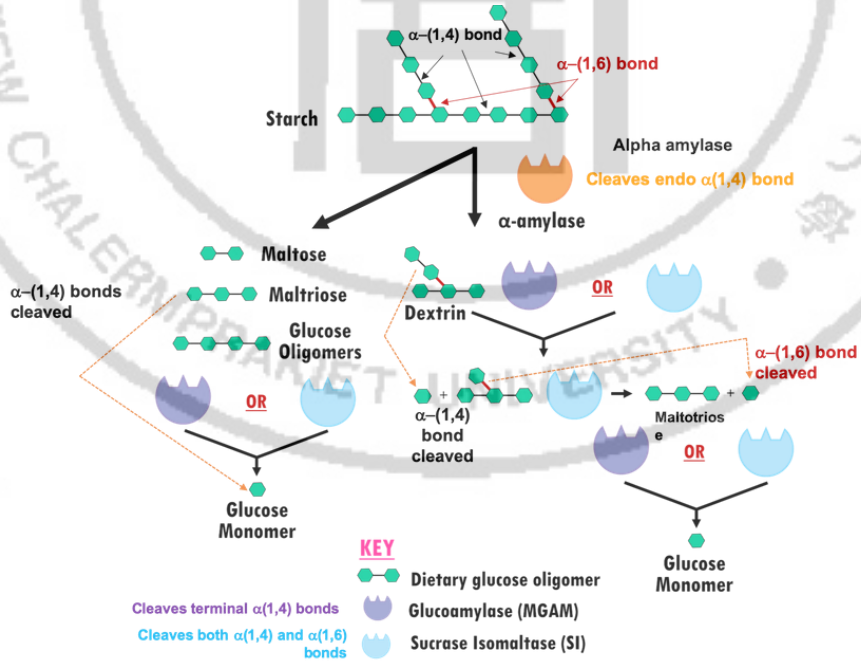

Figure 2.1 Starch digestion by α-amylases and α-glucosidases. Glucose units are shown as green hexagons (46).

2.3 α-Glucosidase inhibitors

α-Glucosidase inhibitors can be used as a first-line drug in newly diagnosed type 2 diabetes insufficiently treated with diet and exercise alone, as well as in combination with all oral antidiabetics and insulin if monotherapy with these drugs fails to achieve the targets for HbA_{1c} and post-prandial blood glucose (47). α-Glucosidase inhibitors, such as acarbose, miglitol and voglibose, which are carbohydrate mimetics or derivatives, have already been marketed for the treatment of type II diabetes mellitus. These drug molecules can decrease postprandial hyperglycemia and hyperinsulinemia, introducing gastrointestinal adverse effects including diarrhea, flatulence and abdominal discomfort. Developing more efficient and safer inhibitors for hyperglycemia control in diabetes remains a global health priority. Acarbose is a well-known, natural product that inhibits α-amylases and α-glucosidases. The binding of carbose to α-glucosidases prevents cleavage of dietary starch and oligosaccharides, resulting in reduced monosaccharide formation and lowering postprandial blood glucose levels (5). It is a competitive inhibitor with a high affinity for sucrase and a lesser affinity for glucoamylase and pancreatic α-amylase in humans (48).

In addition to α-glucosidase inhibitors, such as acarbose, miglitol and voglibose, it was also found that flavonoid compounds such as luteolin and naringenin have been reported to act as potential glucosidase inhibitors that provide protective effects in diabetes therapy both *in vitro* and *in vivo* (5). Moreover, Yeast α-glucosidase is potently inhibited by the anthocyanidin, isoflavone, and flavonol groups with IC_{50} values less than 15 μM. Rat's small intestinal α-glucosidase is weakly inhibited by many flavonoids and slightly by the anthocyanidin and isoflavone groups (46).

CHAPTER III

EXPERIMENTAL

3.1 Chemical experimental

A. Equipment and chemicals

3.1.1 Equipment

Analytical balance model ML204	Mettler Toledo, Switzerland
Magnetic stirrer	Heidolph, Germany
Rotary evaporator	Buchi, Japan

3.1.2 Chemicals

DBU (1,8-diazabicyclo[5,4,0]undec-7-ene)	Fluka, Switzerland
3-Chlorobenzoyl chloride	Aldrich, USA
3,4-Dichlorobenzoyl chloride	Aldrich, USA
3,4-Difluorobenzoyl chloride	Aldrich, USA
2,4-Dihydroxyacetophenone	Aldrich, USA
2,5-Dihydroxyacetophenone	Aldrich, USA
3,5-Dinitrobenzoyl chloride	Aldrich, USA
Ethyl acetate	J.T Baker, USA
4-Fluorobenzoyl chloride	Aldrich, USA
Hexane	J.T Baker, USA
Hydrochloric acid	E. Merck, Germany
Methanol	J.T Baker, USA
3-Methoxybenzoyl chloride	Aldrich, USA
4-Methoxybenzoyl chloride	Aldrich, USA
4-Nitrobenzoyl chloride	Aldrich, USA
Pyridine	Labscan, Thailand
Silica gel F_{254} (0.2 mm.)	E. Merck, Germany
Silica gel 60 No. 1.07734	E. Merck, Germany
Sodium hydroxide	Ajax Finechem, Australia

Sodium sulfate anhydrous	Fischer Scientific, UK
2,3,4-Trihydroxyacetophenone	Aldrich, USA
2,4,6-Trihydroxyacetophenone	Aldrich, USA

B. Methods

The eighteen chromone compounds were synthesized using the previously reported synthesis pathways (49) to increase the yield for α-glucosidase inhibitory activity evaluation. The cyclization of phenolic ketones was carried out in one step by reacting with aroyl chloride in the presence of DBU, outlined as shown in Scheme 1. The intermediate chromone ester was then hydrolyzed to yield the desired chromone derivatives.

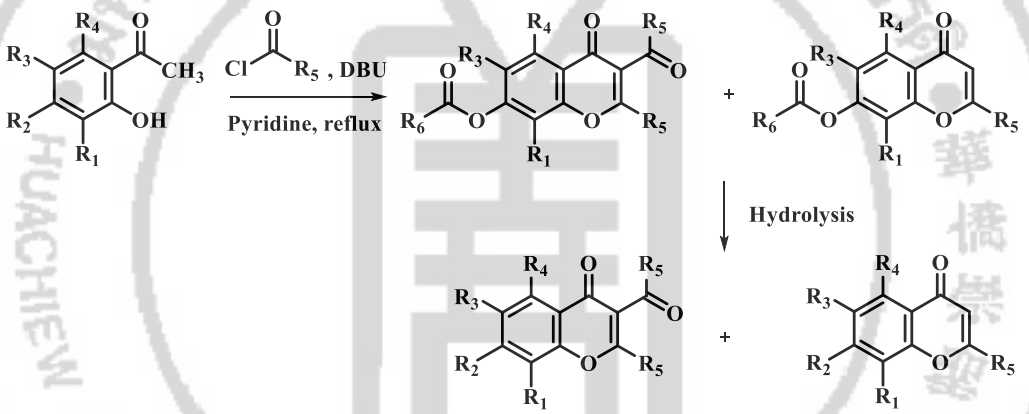

Scheme 1. Synthesis of chromone derivatives.

The synthesized compounds were purified by column chromatography and/or recrystallization. The compounds were identified by Thin layer chromatography (TLC) on silica gel GF_{254} coated aluminum sheets 20x20 cm (E. Merck) with spots visualized by UV light (254 nm).

1. 7-Hydroxy-2-(4'-fluorophenyl) chromone 12.

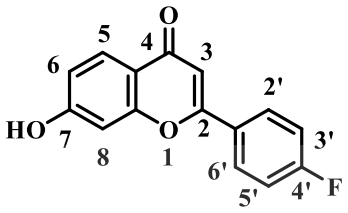

To a stirred solution of 2,4-dihydroxyacetophenone (0.5 g, 3.29 mmol) in pyridine (20 mL) was slowly added 4-fluorobenzoyl chloride (0.8 mL, 6.81 mmol) and then DBU (1.0 mL, 6.69 mmol). The reaction mixture was refluxed at 120-140 °C for 24 hours, and pyridine was evaporated in vacuo. The mixture was poured into 5 mL of concentrated HCl in 100 mL water and extracted with ethyl acetate (2 x 50 mL). The combined organic layers were washed with water (2 x 50 mL), dried over anhydrous sodium sulfate, and filtered. After evaporation, the crude product was hydrolyzed by a mixture of dioxane (2 mL), methanol (4 mL), water (1 mL) and 10 % NaOH (2 mL). The mixture was stirred at room temperature for 3-4 hours. The reaction mixture was acidified with 4N HCl, poured into 50 mL water, and then extracted with ethyl acetate (2 x 50 mL). The combined organic layers were washed with water (2 x 50 mL), dried over anhydrous sodium sulfate, and filtered. After evaporation, the crude product was purified by column chromatography (ethyl acetate/hexane [1:1] to provide the yellow solid (316.2 mg, 37.51%); TLC (silica gel GF 254, ethyl acetate/hexane [1:1]). R_f of 2,4-dihydroxyacetophenone = 0.61, compound **12** = 0.45.

2. 7-Hydroxy-2-(3',5'-dinitrophenyl) chromone 13.

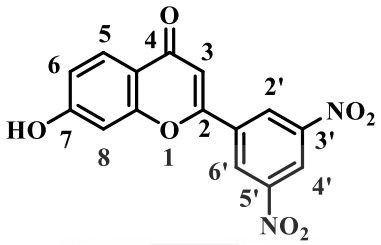

Compound **13** was synthesized using the same procedure as described for compound **12** from 2,4-dihydroxyacetophenone (0.5 g, 3.29 mmol), 3,5-dinitrobenzoyl chloride (1.0 g, 4.34 mmol) and DBU (1.0 mL, 6.69 mmol). After hydrolysis and purification by column chromatography (ethyl acetate/hexane [1:1]), the desired compound **8** was obtained as a yellow solid (184.9 mg, 17.12%); TLC (silica gel GF 254, ethyl acetate/ hexane [1:1]). R_f of 2,4-dihydroxyacetophenone = 0.61, compound **13** = 0.39.

3. 7-Hydroxy-2-(3'-chlorophenyl) chromone 14.

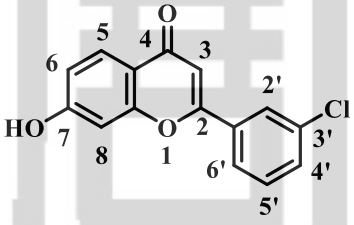

Compound **14** was synthesized using the same procedure as described for compound **12** from 2,4-dihydroxyacetophenone (0.5 g, 3.29 mmol), 3-chlorobenzoyl chloride (0.8 mL, 6.32 mmol) and DBU (1.0 mL, 6.69 mmol). After hydrolysis and purification by column chromatography (ethyl acetate/hexane [1:1]), the desired compound **14** was obtained as a yellow solid (105.2 mg, 11.73%); TLC (silica gel GF 254, ethyl acetate/hexane [1:1]). R_f of 2,4-dihydroxyacetophenone = 0.61, compound **14** = 0.40.

4. 7-Hydroxy-2-(3',4'-dichlorophenyl) chromone 15.

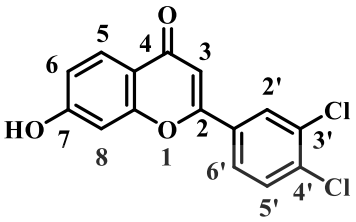

Compound **15** was synthesized using the same procedure as described for compound **12** from 2,4-dihydroxyacetophenone (0.5 g, 3.29 mmol), 3,4-dichlorobenzoyl chloride (1.0 g, 4.77 mmol) and DBU (1.0 mL, 6.69 mmol). After hydrolysis and purification by column chromatography (ethyl acetate/hexane [1:1]), the desired compound **15** was obtained as a yellow solid (215.4 mg, 21.32%); TLC (silica gel GF 254, ethyl acetate/hexane [1:1]). R_f of 2,4-dihydroxyacetophenone = 0.61, compound **15** = 0.45.

5. 5,7-Dihydroxy-2-(4'-fluorophenyl) chromone 18.

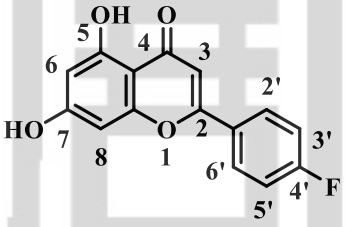

Compound **18** was synthesized using the same procedure as described for compound **12** from 2,4,6-trihydroxyacetophenone (0.5 g, 2.69 mmol), 4-fluorobenzoyl chloride (0.8 mL, 6.81 mmol) and DBU (1.0 mL, 6.69 mmol). After hydrolysis and purification by column chromatography (ethyl acetate/hexane [1:1]), the desired compound **18** was obtained as a yellow solid (344.0 mg, 46.98%); TLC (silica gel GF 254, ethyl acetate/hexane [1:1]). R_f of 2,4,6-trihydroxyacetophenone = 0.69, compound **18** = 0.85.

6. 5,7-Dihydroxy-2-(3',4'-difluorophenyl) chromone 19.

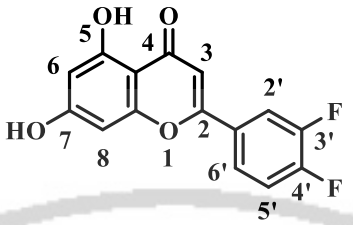

Compound **19** was synthesized using the same procedure as described for compound **12** from 2,4,6-trihydroxyacetophenone (0.5 g, 2.69 mmol), 3,4-difluorobenzoyl chloride (0.8 mL, 6.36 mmol) and DBU (1.0 mL, 6.69 mmol). After hydrolysis and purification by column chromatography (ethyl acetate/hexane [1:1]), the desired compound **19** was obtained as a yellow solid (182.8 mg, 23.42%); TLC (silica gel GF 254, ethyl acetate/hexane [1:1]). R_f of 2,4,6-trihydroxyacetophenone = 0.69, compound **19** = 0.84.

7. 5,7-Dihydroxy-2-(3'-chlorophenyl) chromone 23.

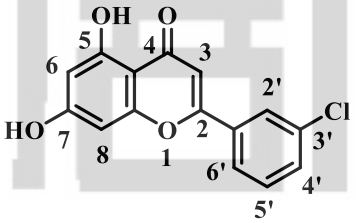

Compound **23** was synthesized using the same procedure as described for compound **12** from 2,4,6-trihydroxyacetophenone (0.5 g, 2.69 mmol), 3-chlorobenzoyl chloride (0.8 mL, 6.32 mmol) and DBU (1.0 mL, 6.69 mmol). After hydrolysis and purification by column chromatography (ethyl acetate/hexane [1:1]), the desired compound **23** was obtained as a yellow solid (445.6 mg, 57.38%); TLC (silica gel GF 254, ethyl acetate/hexane [1:1]). R_f of 2,4,6-trihydroxyacetophenone = 0.69, compound **23** = 0.87.

8. 5,7-Dihydroxy-2-(3',4'-dichlorophenyl) chromone 24.

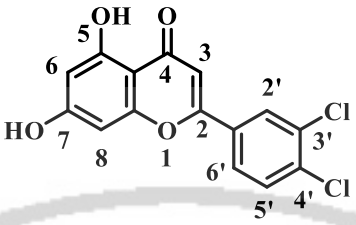

Compound **24** was synthesized using the same procedure as described for compound **12** from 2,4,6-trihydroxyacetophenone (0.5 g, 2.69 mmol), 3,4-dichlorobenzoyl chloride (1.0 g, 4.77 mmol) and DBU (1.0 mL, 6.69 mmol). After hydrolysis and purification by column chromatography (ethyl acetate/hexane [1:1]), the desired compound **24** was obtained as a yellow solid (427.9 mg, 49.23%); TLC (silica gel GF 254, ethyl acetate/hexane [1:1]). R_f of 2,4,6-trihydroxyacetophenone = 0.69, compound **24** = 0.82.

9. 5,7-Dihydroxy-2-(4'-methoxyphenyl) chromone 25.

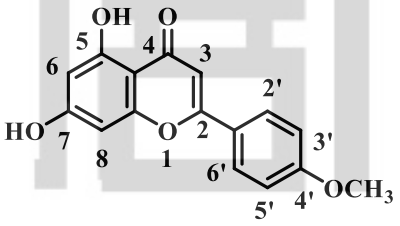

Compound **25** was synthesized using the same procedure as described for compound **12** from 2,4,6-trihydroxyacetophenone (0.5 g, 2.69 mmol), 4-methoxybenzoyl chloride (0.8 mL, 5.51 mmol) and DBU (1.0 mL, 6.69 mmol). After hydrolysis and purification by column chromatography (ethyl acetate/hexane [1:1]), the desired compound **25** was obtained as a yellow solid (319.8 mg, 41.82%); TLC (silica gel GF 254, ethyl acetate/hexane [1:1]). R_f of 2,4,6-trihydroxyacetophenone = 0.69, compound **25** = 0.81.

10. 5,7-Dihydroxy-2-(3'-methoxyphenyl) chromone 26.

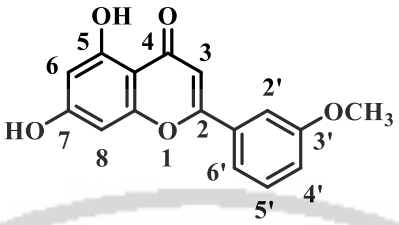

Compound **26** was synthesized using the same procedure as described for compound **12** from 2,4,6-trihydroxyacetophenone (0.5 g, 2.69 mmol), 3-methoxybenzoyl chloride (0.8 mL, 5.51 mmol) and DBU (1.0 mL, 6.69 mmol). After hydrolysis and purification by column chromatography (ethyl acetate/hexane [1:1]), the desired compound **26** was obtained as a yellow solid (227.4 mg, 29.74%); TLC (silica gel GF 254, ethyl acetate/hexane [1:1]). R_f of 2,4,6-trihydroxyacetophenone = 0.69, compound **26** = 0.82.

11. 7,8-Dihydroxy-2-(4'-fluorophenyl)-3-(4"-fluorobenzoyl) chromone 35.

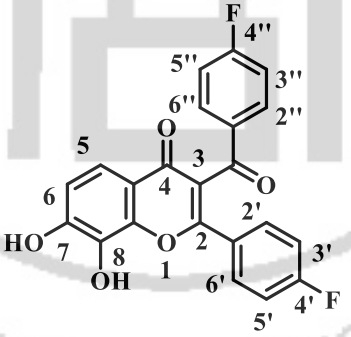

Compound **35** was synthesized using the same procedure as described for compound **12** from 2,3,4-trihydroxyacetophenone (0.5 g, 2.97 mmol), 4-fluorobenzoyl chloride (1.0 mL, 8.51 mmol) and DBU (1.0 mL, 6.69 mmol). After hydrolysis and purification by column chromatography (ethyl acetate/hexane [1:1]), the desired compound **35** was obtained as a yellow solid (150.4 mg, 12.84%); TLC (silica gel GF 254, ethyl acetate/hexane [1:1]). R_f of 2,3,4-trihydroxyacetophenone = 0.56, compound **35** = 0.35.

12. 7,8-Dihydroxy-2-(4'-nitrophenyl)-3-(4"-nitrobenzoyl) chromone 36.

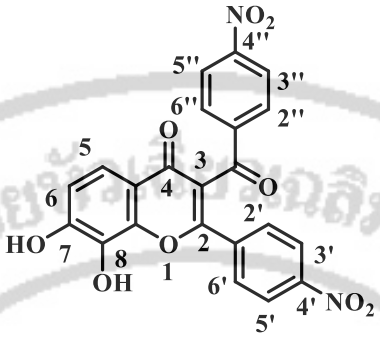

Compound **36** was synthesized using the same procedure as described for compound **12** from 2,3,4-trihydroxyacetophenone (0.5 g, 2.97 mmol), 4-nitrobenzoyl chloride (1.2 g, 6.47 mmol) and DBU (1.0 mL, 6.69 mmol). After hydrolysis and purification by column chromatography (ethyl acetate/hexane [1:1]), the desired compound **36** was obtained as a yellow solid (182.7 mg, 13.72%); TLC (silica gel GF 254, ethyl acetate/hexane [1:1]). R_f of 2,3,4-trihydroxyacetophenone = 0.56, compound **36** = 0.39.

13. 7-Hydroxy-2-(3,4'-difluorophenyl)-3-(3,4"-difluorobenzoyl) chromone 38.

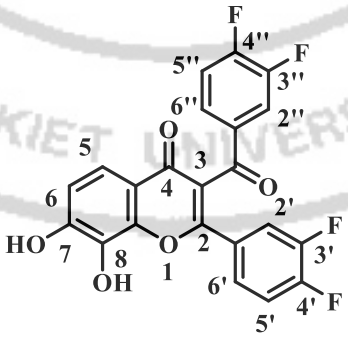

Compound **38** was synthesized using the same procedure as described for compound **12** from 2,3,4-trihydroxyacetophenone (0.5 g, 2.97 mmol), 3,4-difluorobenzoyl chloride (1.0 mL, 7.95 mmol) and DBU (1.0 mL, 6.69 mmol). After hydrolysis and purification by column chromatography (ethyl acetate/hexane [1:1]),

the desired compound **38** was obtained as a yellow solid (224.1 mg, 15.83%); TLC (silica gel GF 254, ethyl acetate/hexane [1:1]). R_f of 2,3,4-trihydroxyacetophenone = 0.56, compound **38** = 0.40.

14. 7-Hydroxy-2-(3'-methoxyphenyl)-3-(3"-methoxybenzoyl) chromone 41.

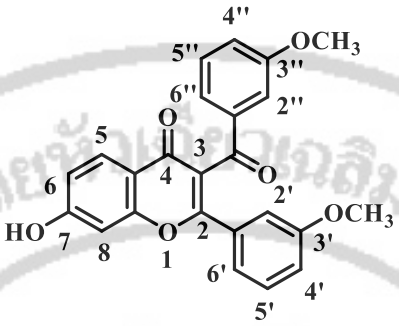

Compound **41** was synthesized using the same procedure as described for compound **12** from 2,4-dihydroxyacetophenone (0.5 g, 3.29 mmol), 3-methoxybenzoyl chloride (1.0 mL, 7.12 mmol) and DBU (1.0 mL, 6.69 mmol). After hydrolysis and purification by column chromatography (ethyl acetate/hexane [1:1]), the desired compound **41** was obtained as a yellow solid (217.8 mg, 16.45%); TLC (silica gel GF 254, ethyl acetate/hexane [1:1]). R_f of 2,4-dihydroxyacetophenone = 0.61, compound **41** = 0.52.

15. 7-Hydroxy-2-(4'-fluorophenyl)-3-(4"-fluorobenzoyl) chromone 42.

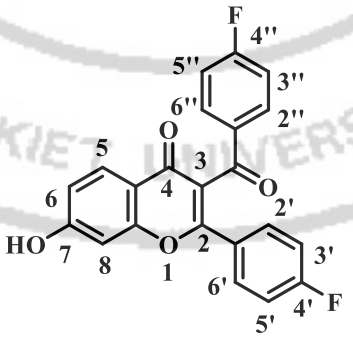

Compound **42** was synthesized using the same procedure as described for compound **12** from 2,4-dihydroxyacetophenone (0.5 g, 3.29 mmol), 4-fluorobenzoyl chloride (1.0 mL, 8.51 mmol) and DBU (1.0 mL, 6.69 mmol). After hydrolysis and purification by column chromatography (ethyl acetate/hexane [1:1]),

the desired compound **42** was obtained as a yellow solid (141.4 mg, 11.36%); TLC (silica gel GF 254, ethyl acetate/hexane [1:1]). R_f of 2,4-dihydroxyacetophenone = 0.61, compound **42** = 0.50.

16. 7-Hydroxy-2-(4'-nitrophenyl)-3-(4"-nitrobenzoyl) chromone 43.

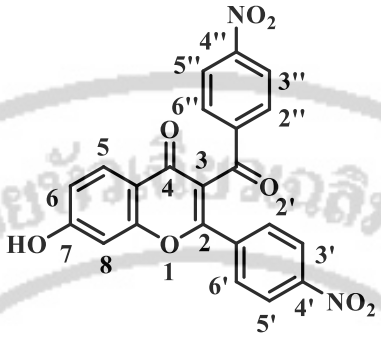

Compound **43** was synthesized using the same procedure as described for compound **12** from 2,4-dihydroxyacetophenone (0.5 g, 3.29 mmol), 4-nitrobenzoyl chloride (1.2 g, 6.47 mmol) and DBU (1.0 mL, 6.69 mmol). After hydrolysis and purification by column chromatography (ethyl acetate/hexane [1:1]), the desired compound **43** was obtained as a yellow solid (95.6 mg, 6.72%); TLC (silica gel GF 254, ethyl acetate/hexane [1:1]). R_f of 2,4-dihydroxyacetophenone = 0.61, compound **43** = 0.54.

17. 7-Hydroxy-2-(4'-methoxyphenyl)-3-(4"-methoxybenzoyl) chromone 44.

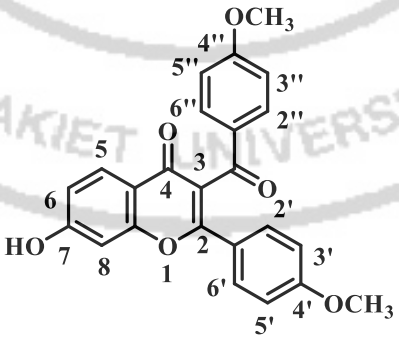

Compound **44** was synthesized using the same procedure as described for compound **12** from 2,4-dihydroxyacetophenone (0.5 g, 3.29 mmol), 4-methoxybenzoyl chloride (1.0 ml, 7.12 mmol) and DBU (1.0 mL, 6.69 mmol). After hydrolysis and purification by column chromatography (ethyl acetate/hexane [1:1]),

the desired compound **44** was obtained as a yellow solid (495.3 mg, 37.41%); TLC (silica gel GF 254, ethyl acetate/hexane [1:1]). R_f of 2,4-dihydroxyacetophenone = 0.61, compound **44** = 0.51.

18. 5,7-Dihydroxy-2-(4'-nitrophenyl)-3-(4"-nitrobenzoyl) chromone 47.

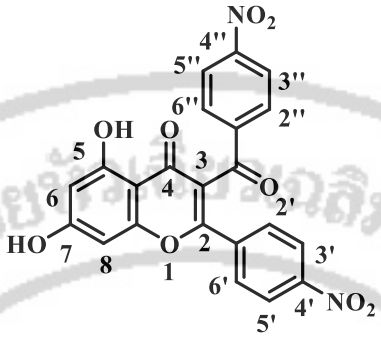

Compound **47** was synthesized using the same procedure as described for compound **12** from 2,4,6-trihydroxyacetophenone (0.5 g, 2.69 mmol), 4-nitrobenzoyl chloride (1.2 g, 6.47 mmol) and DBU (1.0 mL, 6.69 mmol). After hydrolysis and purification by column chromatography (ethyl acetate/hexane [1:1]), the desired compound **47** was obtained as a yellow solid (69.7 mg, 5.78%); TLC (silica gel GF 254, ethyl acetate/hexane [1:1]). R_f of 2,4,6-trihydroxyacetophenone = 0.69, compound **47** = 0.76.

3.2 Biological experimental

A. Equipment and chemicals

3.2.1 Equipment

Analytical balance model M204	Mettler Toledo, Switzerland
Flat bottom 96-well plate	Extra Gene, Taiwan
Microcentrifuge tube 0.5, 1.5 mL	Extra Gene, Taiwan
Micropipettes 0.1-2.5, 2-20, 20-200 µL	Thermo Scientific, USA
Micropipette 1,000 µL	Thermo Scientific, USA
Micropipette tips 10 µL, 200, 1,000 µL	Extra Gene, Taiwan
pH meter model S20K	Mettler teledo, Switzerland
UV-Visible microplate reader	Biochrom, UK
Vortex mixer	Scientific Industries, USA

3.2.2 Chemicals

α-glucosidase enzyme	Sigma, USA
Dimethylsulfoxide (DMSO)	Sigma, USA
Monobasic potassium phosphate	Ajax Finechem, Australia
p-nitrophenyl-α-d-glucopyranoside	E. Merck, Germany
Sodium carbonate	Ajax Finechem, Australia
Sodium hydroxide	Ajax Finechem, Australia

3.2.3 Software

Graphpad Prism 5	Graphpad Software, USA

B. Methods

***In vitro* α-glucosidase inhibitory activity evaluation**

1. Inhibition of α-glucosidase

Forty-one chromone compounds were evaluated for their α-glucosidase inhibitory activity at 30 μM. In brief, 10 μL of α-glucosidase enzyme solution (1 U/mL) is diluted with 120 μL of 0.1 M phosphate buffer (pH 6.8). Then 5 μL of the compound solution prepared in DMSO with various concentrations is added to the enzyme solution. The mixture is then incubated at 37 °C for 15 min. Afterward, 20 μL of 5 mM substrate p-nitrophenyl-α-d-glucopyranoside in phosphate buffer (pH 6.8) are added and incubated for an additional 30 min at 37 °C. The reaction is quenched using 80 μL of 0.2 M Na_2CO_3. Measuring the absorption at a wavelength of 405 nm using a UV spectrophotometer (5). The reaction without enzyme is used as a blank, and each experiment is triplicated. Control is the reaction without an inhibitor. Acarbose was used as a positive control. The inhibitory activity is calculated using the following equation:

Inhibition (%) = [(Control absorption – Sample absorption)/Control absorption] x 100

Where control absorption was the absorption of the reaction without an inhibitor, sample absorption was the absorption of the reaction with chromone compound (inhibitor).

2. Determinations of IC_{50} value

Sixteen most potent chromone compounds (Compounds **19-20**, **23-24, 32-38, 40,** and **42-45**) and a clinical-used α-glucosidase inhibitor (acarbose) were selected to determine the IC_{50} values. The IC_{50} value was calculated from the log dose-response curve plotted between the logarithm of six concentrations and % inhibition using Graphpad Prism 5. The reported IC_{50} values were the average of the three independent experiments, each of which was performed in triplicate.

3.3 Molecular modeling experimental

A. Materials

3.3.1 Computers

Internet network, silicon graphics SGI Iris R800

Silicon Graphics SGI O2 Webforce R5000 SC

Personal computer (PC) Intel core i5

3.3.2 Softwares

AutoDock 4.2 for Windows

SYBYL software version x2.0

B. Methods

The molecular docking calculations were performed using AutoDock version 4.2 (The Scripps Research Institute, Molecular Graphics Laboratory, Department of Molecular biology, CA, USA). The docking study was carried out using the Lamarckian genetic algorithm, applying a standard protocol as shown in Table 3.1. One hundred independent docking runs were carried out for each ligand. Results differing by less than 2.0 Å in positional root-mean-square deviation (RMSD) were clustered together and represented by the result with the most favorable free energy of binding. The docking results, binding mode and binding free energy were analyzed to evaluate the interaction between the ligand and the amino acid residues of α-glucosidase.

Ligand preparation: The molecular structures of active chromone compounds were constructed using the standard parameters of the molecular

modeling software package SYBYLx2.0 (Tripos Associates, Saint Louis, MO, USA). Geometrical optimization was performed using the Powell method with a root-mean-squared (RMS) energy gradient of 0.05 kcal/mol.Å. A tripos force field with Gasteiger-Hückel charges was employed during the energy minimization.

Table 3.1 Docking parameters for α-glucosidase.

Parameters	COX-1 and COX-2
Number of GA run	100
Population size	150
Maximum number of energy evaluations	2,500,000
Maximum number of generation	27,000
Maximum number of top individuals that automatically survive	1
Rate of gene mutation	0.02
Rate of crossover	0.8
Mean of Cauchy distribution for gene mutation	0.0
Variance of Cauchy distribution for gene mutation	1.0
Number of generation for picking worst individual	10

Receptor preparation: The crystal structures of α-glucosidase (PDB codes 3A4A, Table 3.2) complexed with α-D-glucopyranose were retrieved from the Brookhaven Protein Data Bank (http://www.rcsb.org/pdb). The protein templates were prepared for docking study by removing all the native ligand structures and all water molecules from the complex structures. The polar hydrogen atoms were added, and Gasteiger charges were assigned to protein atoms.

Re-docking was carried out for α-glucosidase because only one α-glucosidase crystal structure was available in Protein Data Bank.

Table 3.2 The structures of α-glucosidase complexed with α-D-glucopyranose in the crystal structures.

PDB code	Inhibitor	Structure
1EQG	α-D-glucopyranose	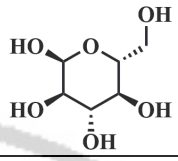

The RMSD value of the best cluster conformation from α-glucosidase re-docking validation was 0.38.

Grid setup: The grid maps representing the protein in the actual docking process were calculated with AutoGrid. The grids (one for each atom type in the ligand, plus one for electrostatic interactions) were chosen to be sufficiently large to include the active site and significant portions of the surrounding surface. The parameters used for autogrid are shown in Table 3.3.

Table 3.3 Autogrid parameters for α-glucosidase.

	Parameters
PDB code	3A4A
Resolution (Å)	1.6
Num. Grid point in x, y, z	60, 60, 60
Spacing (Å)	0.375
Grid center	center on ligand
Smooth	0.5

CHAPTER IV

RESULTS AND DISCUSSION

4.1 Synthesis

The synthetic pathway of 3-unsubstituted and 3-substituted chromone compounds using one-pot cyclization was outlined in Figures 4.1 and 4.2, respectively. The commercially available phenolic ketones reacted with aroyl chloride in the presence of 1,8-diazabicyclo[5,4,0]undec-7-ene (DBU) to generate the intermediate substituted chromone esters intermediates in one step. These intermediates were then submitted to hydrolysis to yield the desired chromone compounds. %Yield of the synthesized compounds was summarized in Table 4.1.

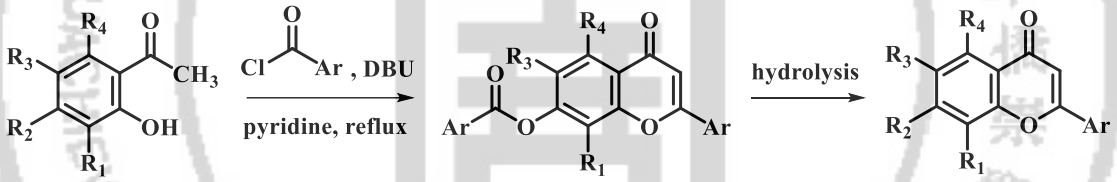

R_1, R_2, R_3, R_4 = OH

Ar = 3-Cl phenyl, 3-OCH_3 phenyl, 4-F phenyl, 4-OCH_3-phenyl, 3,4-diCl phenyl, 3,5-diNO_2 phenyl

Figure 4.1 Synthesis of 3-unsubstituted chromone derivatives.

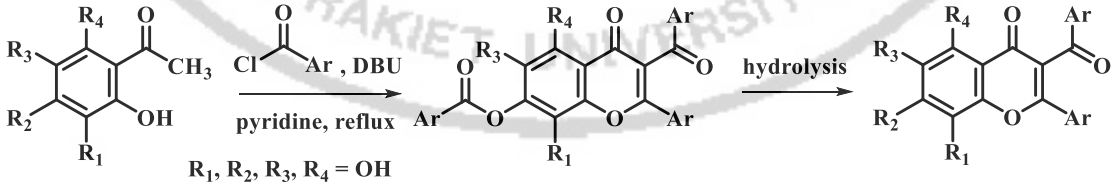

R_1, R_2, R_3, R_4 = OH

Ar = 3-OCH_3 phenyl, 4-F phenyl, 4-OCH_3-phenyl, 4-NO_2-phenyl, 3,4-diF phenyl

Figure 4.2 Synthesis of 3-substituted chromone derivatives.

Table 4.1 %Yield of the synthesized compounds.

Compound	Structure	R_2	%Yield
12	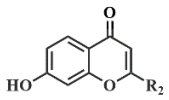	4'-(F)-Phenyl	37.51
13		3', 5'-(diNO_2)-Phenyl	17.12
14		3'-(Cl)-Phenyl	11.73
15		3', 4'-(diCl)-Phenyl	21.32
18	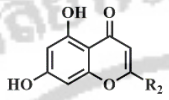	4'-(F)-Phenyl	46.98
19		3', 4'-(diF)-Phenyl	23.42
23		3'-(Cl)-Phenyl	57.38
24		3', 4'-(diCl)-Phenyl	49.23
25		4'-(OCH_3)-Phenyl	41.82
26		3'-(OCH_3)-Phenyl	29.74
35	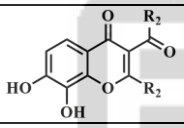	4'-(F)-Phenyl	12.84
36		4'-(NO_2)-Phenyl	13.72
38	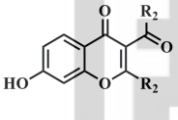	3', 4'-(diF)-Phenyl	15.83
41		3'-(OCH_3)-Phenyl	16.45
42		4'-(F)-Phenyl	11.36
43		4'-(NO_2)-Phenyl	6.72
44		4'-(OCH_3)-Phenyl	37.41
47	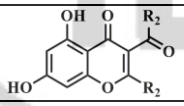	4'-(NO_2)-Phenyl	5.78

4.2 *In vitro* α-glucosidase inhibitory activity

The ability of chromone derivatives to inhibit α-glucosidase was determined. In this assay, α-glucosidase activity is determined by a reaction in which α-glucosidase hydrolyzes *p*-nitrophenyl-α-D-glucopyranoside resulting in the formation of a product proportional to the α-glucosidase activity. The percentage of α-glucosidase inhibition was calculated as follows:

Inhibition (%) = [(Control absorption - Sample absorption)/Control absorption] x 100

Where control absorption was the absorption of the reaction without an inhibitor, sample absorption was the absorption of the reaction with chromone compound (inhibitor).

Forty-one chromone compounds were evaluated for their ability to inhibit α-glucosidase at 30 μM. A clinically-used α-glucosidase inhibitor, acarbose, was used as a positive control. The α-glucosidase inhibitory activities of the 3-unsubstituted and 3-substituted chromone compounds are summarized in Tables 4.2 and 4.3, respectively. Among these compounds, sixteen compounds (compounds **19-20**, **23-24**, **32-38**, **40** and **42-45**) showed higher potency than Acarbose (20.39% inhibition obtained from the same experiment). In general, the 3-unsubstituted derivatives showed 2.38-67.85% inhibition. Most of the 3-substituted chromone compounds displayed > 16.57% inhibition and up to 69.24% inhibition (except compounds **39** and **46-48**). Compound **33** exhibited the highest activity with 69.24% inhibition. Sixteen chromone compounds that exhibited %inhibition in the minus value were inactive. Sixteen most potent chromone compounds (Compounds **19-20, 23-24, 32-38, 40** and **42-45**) and Acarbose were selected to determine the IC_{50} values (Tables 4.2 and 4.3). The IC_{50} value was calculated from the log dose-response curve plotted between the logarithm of six concentrations and %inhibition using Graphpad Prism 5 (Figures 4.2 and 4.3).

Among twenty-four 3-unsubstituted chromone derivatives, compound **24** was the most potent α-glucosidase inhibitor. Compounds **19**, **20**, **23** and **24** were more potent than acarbose with the IC_{50} values 37.00, 37.17, 38.35, 12.42 and 42.34 μM, respectively.

Five 3-substituted chromone derivatives, compounds **33**, **35**, **37**, **38** and **45,** showed higher potency than Acarbose with the IC_{50} values 5.06, 40.55, 38.39, 40.47, 21.71 and 42.34 μM, respectively. Compound **33** was the most potent α-glucosidase inhibitor.

Table 4.2 The *in vitro* α-glucosidase inhibitory activity result of the 3-unsubstituted chromone derivatives.

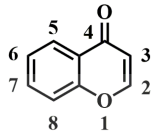

Compound	Structure	R_2	Inhibition (%) ± SD	IC_{50} (μM) ± SD
1	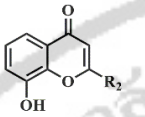	Phenyl	2.38 ± 0.07	-
3	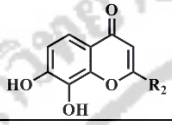	Benzyl	2.44 ± 0.02	-
4		Phenyl	7.58 ± 0.29	-
5	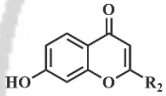	CH_3	-11.43 ± 0.20	-
11		3'-(CF_3)-Phenyl	-20.53 ± 0.32	-
12		4'-(F)-Phenyl	-15.23 ± 0.39	-
13		3', 5'-(diNO_2)-Phenyl	-22.17 ± 0.05	-
14		3'-(Cl)-Phenyl	-24.96 ± 0.66	-
15		3', 4'-(diCl)-Phenyl	6.50 ± 0.18	-
16		4'-(t-butyl)-Phenyl	15.89 ± 0.70	-
17	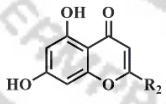	3'-(CF_3)-Phenyl	2.54 ± 0.25	-
18		4'-(F)-Phenyl	2.58 ± 0.04	-
19		3', 4'-(diF)-Phenyl	45.77 ± 0.38	37.00 ± 0.22
20		4'-(t-butyl)-Phenyl	52.78 ± 0.60	37.17 ± 0.06
22		3', 5'-(diNO_2)-Phenyl	-6.24 ± 0.32	-
23		3'-(Cl)-Phenyl	28.44 ± 0.57	38.35 ± 0.05
24		3', 4'-(diCl)-Phenyl	67.85 ± 0.40	12.42 ± 0.13
25		4'-(OCH_3)-Phenyl	17.82 ± 0.78	-
26		3'-(OCH_3)-Phenyl	-12.54 ± 0.31	-
27	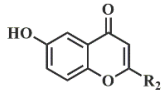	3'-(OCH_3)-Phenyl	-13.42 ± 0.11	-
28		3'-(Cl)-Phenyl	-1.17 ± 0.02	-
29		4'-(F)-Phenyl	-21.85 ± 0.75	-
31		4'-(t-butyl)-Phenyl	-13.68 ± 0.41	-
49	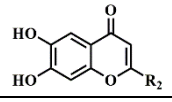	3'-(OCH_3)-Phenyl	-24.84 ± 0.36	-

Acarbose	20.39 ± 0.52	42.34 ± 0.25

Table 4.3 The *in vitro* α-glucosidase inhibitory activity result of 3-substituted chromone derivatives.

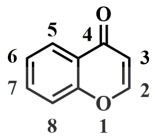

Compound	Structure	R_2	Inhibition (%) ± SD	IC_{50} (μM) ± SD
32	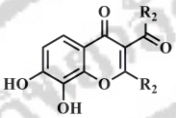	3'-(CF_3)-Phenyl	20.21 ± 0.25	44.14 ± 0.18
33		3'-(Cl)-Phenyl	69.24 ± 0.28	5.06 ± 0.12
34		3'-(OCH_3)-Phenyl	21.20 ± 0.24	48.01 ± 0.38
35		4'-(F)-Phenyl	20.24 ± 0.15	40.55 ± 0.05
36		4'-(NO_2)-Phenyl	23.84 ± 0.44	48.72 ± 0.55
37		4'-(OCH_3)-Phenyl	29.45 ± 0.21	38.39 ± 0.25
38	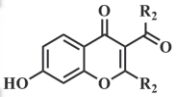	3', 4'-(diF)-Phenyl	21.81 ± 0.50	40.47 ± 0.19
39		3'-(CF_3)-Phenyl	-16.19 ± 0.42	-
40		3'-(Cl)-Phenyl	23.62 ± 0.42	52.27 ± 0.55
41		3'-(OCH_3)-Phenyl	17.99 ± 0.30	-
42		4'-(F)-Phenyl	20.53 ± 0.37	53.35 ± 0.09
43		4'-(NO_2)-Phenyl	28.26 ± 0.29	45.44 ± 0.40
44		4'-(OCH_3)-Phenyl	21.69 ± 0.48	43.88 ± 0.21
45		4'-(t-butyl)-Phenyl	69.08 ± 0.02	21.71 ± 0.19
46	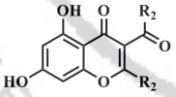	3'-(OCH_3)-Phenyl	-26.39 ± 0.32	-
47		4'-(NO_2)-Phenyl	-24.49 ± 0.41	-
48	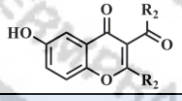	4'-(t-butyl)-Phenyl	-5.59 ± 0.14	-
Acarbose			20.39 ± 0.52	42.34 ± 0.25

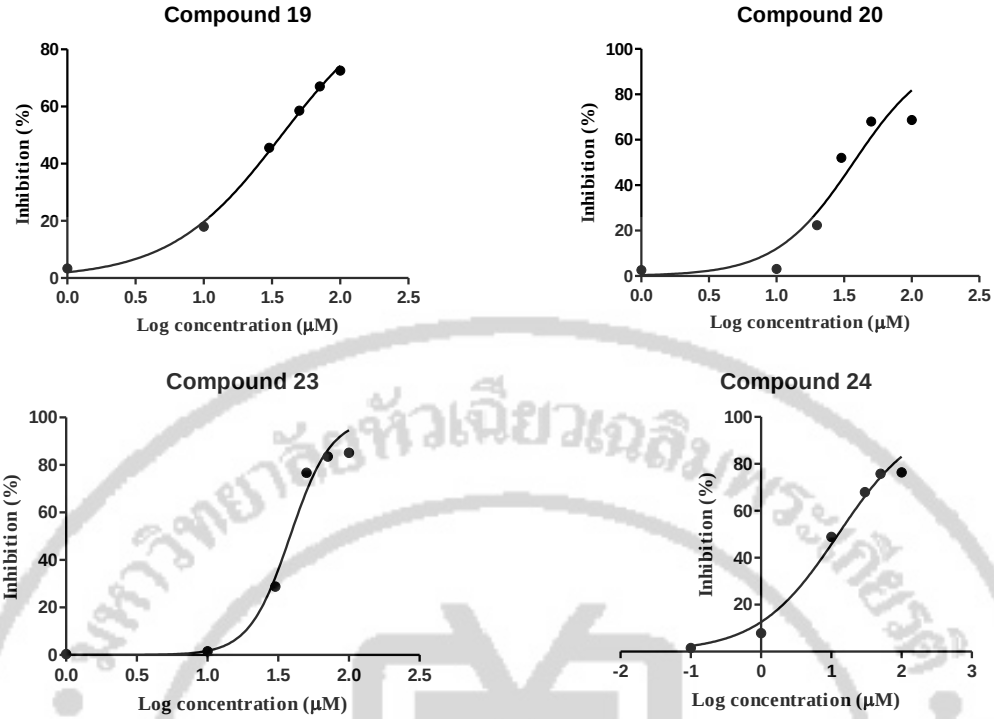

Figure 4.2 The log dose-response curve plotted between the logarithm of six concentrations and %inhibition of the 3-unsubstituted chromone derivatives (compounds **19**-**20** and **23**-**24**).

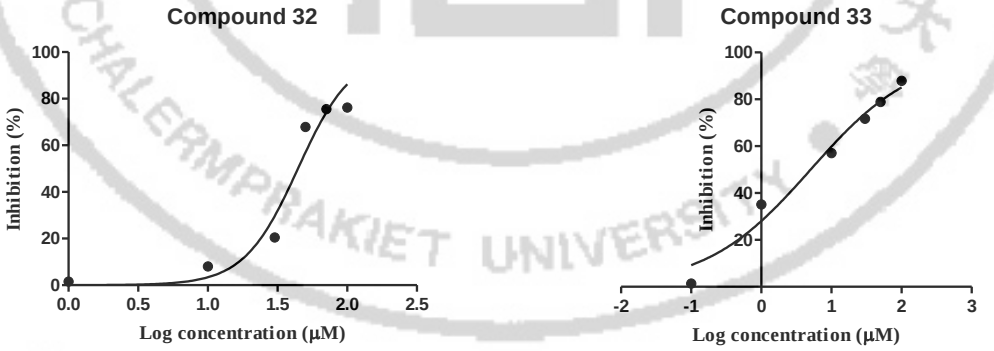

Figure 4.3 The log dose-response curve plotted between the logarithm of six concentrations and %inhibition of the 3-substituted chromone derivatives (compounds **32**-**38**, **40** and **42**-**45**).

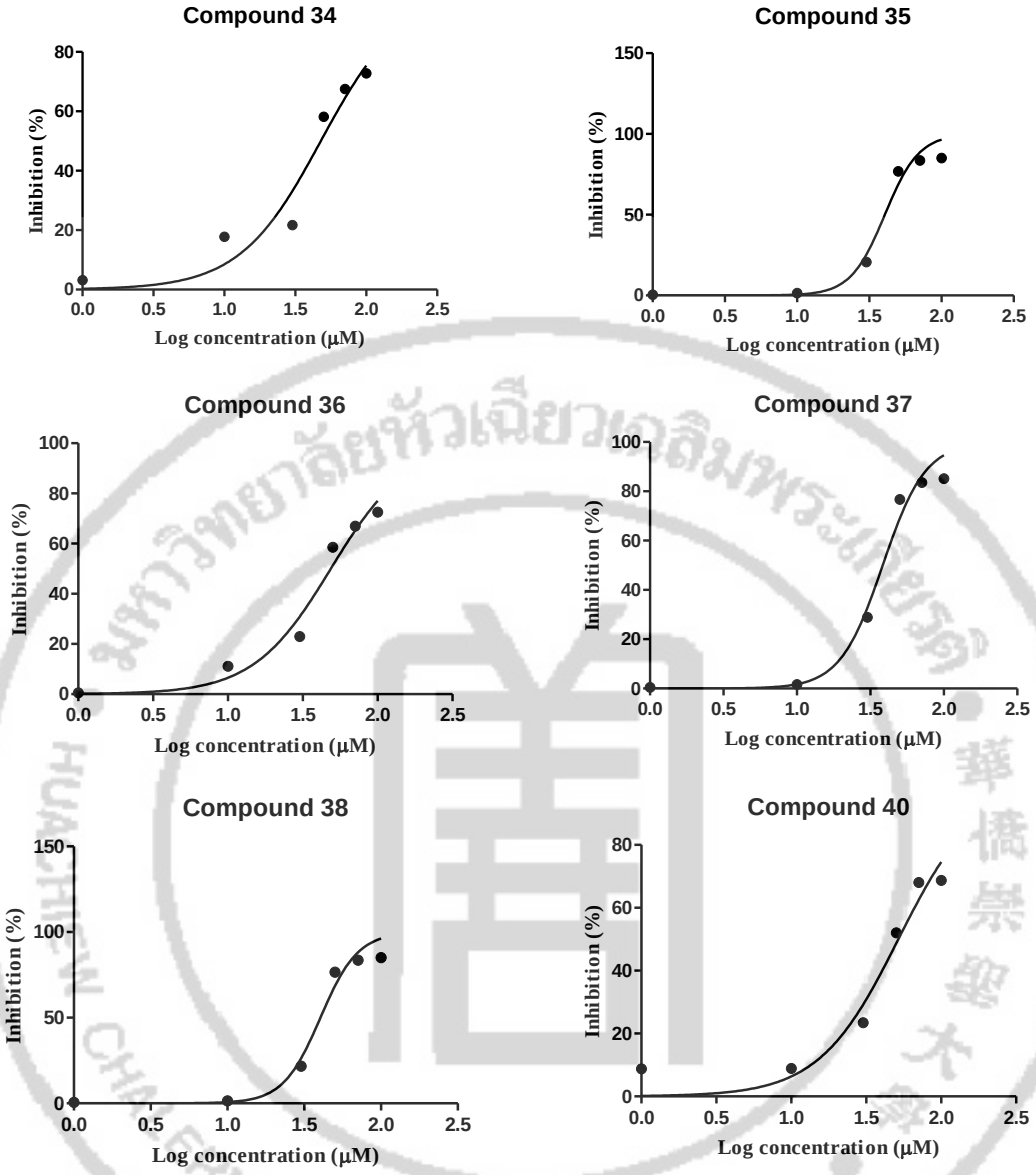

Figure 4.3 (continued) The log dose-response curve plotted between the logarithm of six concentrations and %inhibition of the 3-substituted chromone derivatives (compounds **32**-**38**, **40** and **42**-**45**).

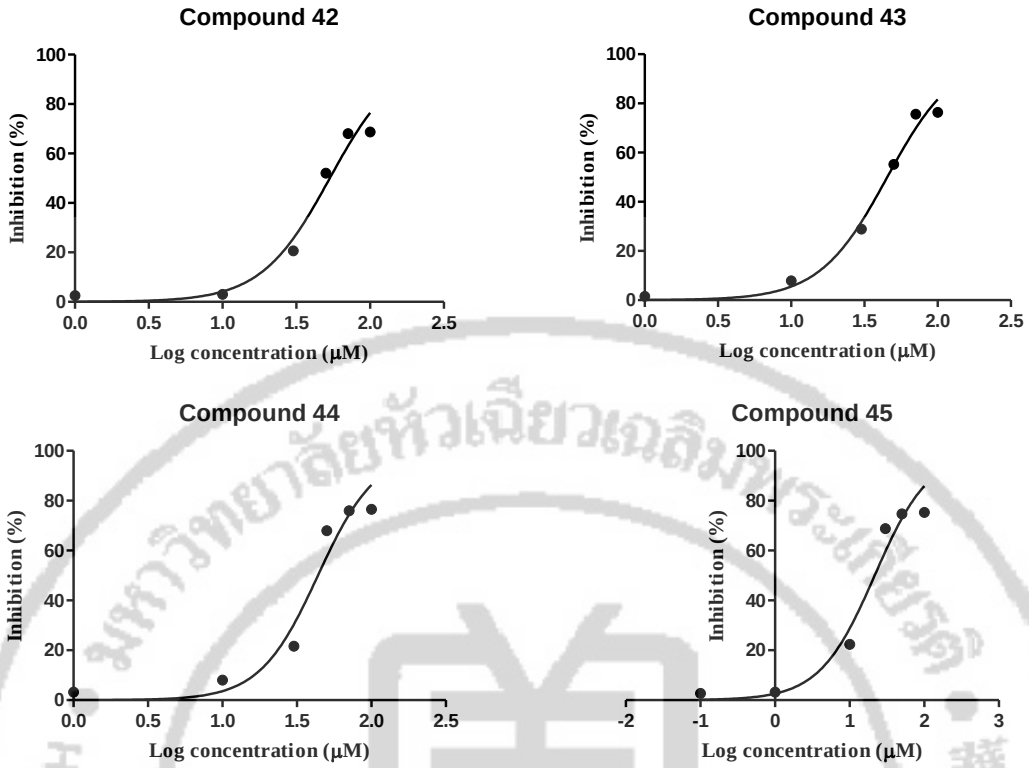

Figure 4.3 (continued) The log dose-response curve plotted between the logarithm of six concentrations and %inhibition of the 3-substituted chromone derivatives (compounds **32-38**, **40** and **42-45**).

Among selected sixteen compounds, nine compounds (compounds **19-20**, **23-24**, **33**, **35, 37-38** and **45**) exhibited greater potency than Acarbose 1.05-8.37 times as shown in blue color in Figure 4.4. In contrast, seven compounds (compounds **32**, **34**, **36**, **40** and **42-45**) with lower potency than acarbose 0.79-0.96 times were presented in red color in Figure 4.4. The potency ratio of each chromone compound compared with Acarbose was calculated as follows:

The potency ratio = The IC_{50} value of Acarbose/The IC_{50} value of chromone

Compounds **33** and **24** were the two most potent α-glucosidase inhibitors with IC_{50} values of 5.06 and 12.42 μM, respectively.

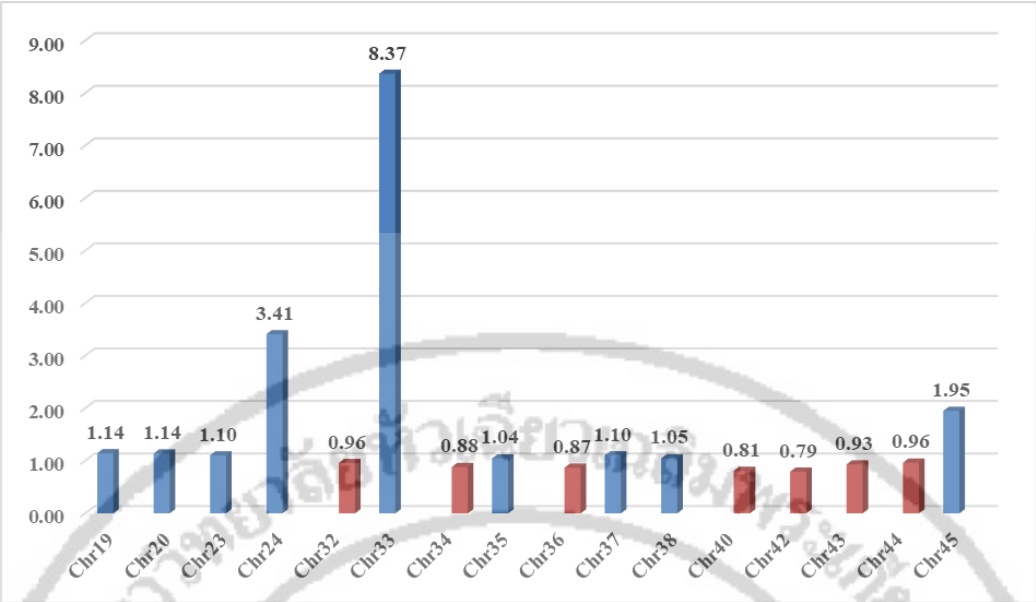

Figure 4.4 The potency ratio of chromone compounds compared with acarbose. Chromone compounds (Chr) with greater potency than Acarbose displayed values of more than one (blue). Chromone compounds with lower potency exhibited a potency ratio of less than one (red).

4.3 Docking simulation study of chromone compounds against α-glucosidase

To obtain the interaction between chromone compounds and α-glucosidase, twenty-five active chromone compounds (compounds which exhibited %inhibition in the positive value) were docked with α-glucosidase using AutoDock 4.2. The crystal structure of α-glucosidase (PDB code 3A4A) was used to evaluate the interaction between the chromone compounds against α-glucosidase templates. Conformations of the ligands evaluated with the AutoDock 4.2 program were allowed to be flexible while the macromolecule target was fixed. The docking parameters and settings were given in the molecular modeling experimental chapter. The docking results were reported as binding energy. The lower the binding energy, the higher the binding affinity. Table 4.4 shows the binding energies of chromone derivatives against α-glucosidase.

Table 4.4 The binding energies of chromone derivatives docked with α-glucosidase.

Compounds	Binding energy (kcal/mole)	Compounds	Binding energy (kcal/mole)
3-Unsubstituted chromones		3-Substituted chromones	
1	-6.93	32	-7.72
3	-7.21	33	-8.41
4	-6.65	34	-8.17
15	-7.32	35	-7.19
16	-7.26	36	-7.89
17	-7.05	37	-7.71
18	-6.52	38	-8.13
19	-6.34	40	-8.82
20	-7.31	41	-8.25
23	-7.32	42	-7.62
24	-7.09	43	-9.12
25	-6.23	44	-7.71
		45	-9.01
Acarbose	-9.91		

As shown in Table 4.4, the docking results agreed with the experimental α-glucosidase inhibitory data. The 3-substituted chromones exhibited higher binding energy against α-glucosidase (binding energy between -7.19 and -9.12 kcal/mole) than the 3-unsubstituted compounds (binding energy between -6.23 and -7.32 kcal/mole).

มหาวิทยาลัยหัวเฉียวเฉลิมพระเกียรติ
華僑崇聖大學
HUACHIEW CHALERMPRAKIET UNIVERSITY

CHAPTER VII

CONCLUSION

In this study, chromone compounds are expected to act as potential α-glucosidase inhibitors. Forty-one chromone compounds were evaluated for the inhibitory activity against α-glucosidase at the concentration of 30 μM compared with the positive control, Acarbose. Among these forty-one compounds, sixteen compounds (compounds **19**-**20**, **23**-**24**, **32**-**38**, **40** and **42**-**45**) exhibited greater inhibitory activity than Acarbose. Twenty-five compounds were active compounds. The 3-unsubstituted derivatives showed 2.38-67.85% inhibition. Most of the 3-substituted chromone compounds displayed > 16.57% inhibition and up to 69.24% inhibition (except compounds **39** and **46**-**48**).

Then, the sixteen most potent chromone compounds (Compounds **19**-**20, 23**-**24, 32**-**38, 40** and **42**-**45**) and Acarbose were selected to determine the IC_{50} values. Among 3-unsubstituted chromone derivatives, compounds **19**, **20**, **23** and **24** were more potent than Acarbose with the IC_{50} values 37.00, 37.17, 38.35, 12.42 and 42.34 μM, respectively. Five 3-substituted chromone derivatives, compounds **33**, **35**, **37**, **38** and **45,** exhibited greater inhibitory activity than Acarbose with the IC_{50} values 5.06, 40.55, 38.39, 40.47, 21.71 and 42.34 μM, respectively. Compounds **33** and **24** were the two most potent α-glucosidase inhibitors with IC_{50} values of 5.06 and 12.42 μM, respectively.

To obtain the interaction between chromone compounds and α-glucosidase, twenty-five active chromone compounds were docked with α-glucosidase (PDB code 3A4A) using AutoDock 4.2. The docking results agreed with the *in vitro* α-glucosidase inhibitory activity assay. The 3-substituted chromones showed higher binding energy against α-glucosidase (binding energy between -7.19 and -9.12 kcal/mole) than the 3-unsubstituted compounds (binding energy between -6.23 and -7.32 kcal/mole).

Therefore, nine compounds (compounds **19**, **20**, **23, 24**, **33**, **35**, **37**, **38** and **45**) that are more potent than Acarbose will be selected for further pre-clinical studies, i.e., *in vivo* activity testing and toxicity testing.

REFERENCES

1. IDF Diabetes Atlas, 6th ed. 2014 update. Brussels, Belgium: International Diabetes Federation, International Diabetes Federation 2014.
2. Guariguata L, Whiting D, Hambleton I, Beagley J, Linnenkamp U, Shaw J. Global estimates of diabetes prevalence for 2013 and projections for 2035. Diabetes Res Clin Pract.2014;103:137-49.
3. Olokoba AB, Obateru OA, Olokoba LB. Type 2 diabetes mellitus: a review of current trends. Oman Med J. 2012;27(4):269-73.
4. Derosacorresponding G, Maffioli P. α-Glucosidase inhibitors and their use in clinical practice. Arch Med Sci. 2012;8(5):899-906.
5. Zhen J, Dai Y, Villani T, Giurleo D, Simon JE, Wu Q. Synthesis of novel flavonoid alkaloids as α-glucosidase inhibitors. Bioorg Med Chem. 2017;25(20):5355-64.
6. Derosa G, Maffioli P. α-Glucosidase inhibitors and their use in clinical practice. Arch Med Sci. 2012;8(5):899–906.
7. Kumar S, Narwal S, Kumar V, Prakash O. α-Glucosidase inhibitors from plants: a natural approach to treat diabetes. Pharmacogn Rev. 2011;5(9):19–29.
8. Panche AN, Diwan AD, Chandra SR. Flavonoids: an overview. J Nutr Sci. 2016;5:e47.
9. Mead JR, McNair N. Antiparasitic activity of flavonoids and isoflavones against *Cryptosporidium parvum* and *Encephalitozoon intestinalis*. FEMS Microbiol Lett. 2006;259(1):153-7.
10. Sharifi-Rad J, Hoseini-Alfatemi SM, Sharifi-Rad M, Teixeira da Silva JA. Antibacterial, antioxidant, antifungal and anti-inflammatory activities of crude extract from *Nitraria schoberi* fruits. Biotech. 2015;5(5):677-84.
11. Ungwitayatorn J, Wiwat C, Samee W, Nunthanavanit P, Phosrithong N. Synthesis, *in vitro* evaluation, and docking studies of novel chromone derivatives as HIV-1 protease inhibitor. J Mol Struct. 2011;1001(1):152-61.

12. Phosrithong N, Samee W, Nunthanavanit P, Nunthanavanit P, Ungwitayatorn J. *In vitro* antioxidant activity study of novel chromone derivatives. Chem Biol Drug Des. 2012;79(6):981-9.
13. Lerdsirisuk P, Maicheen C, Ungwitayatorn J. Antimalarial activity of HIV-1 protease inhibitor in chromone series. Bioorg Chem. 2014;57:142-7.
14. Maicheen C, Jittikoon J, Vajragupta O, Ungwitayatorn J. Synthesis, topoisomerase I inhibitory and cytotoxic activities of chromone derivatives. Med Chem. 2013;9(3):329-39.
15. Desjardins RE, Canfield CJ, Haynes JD, Chulay JD. Quantitative assessment of antimalarial activity *in vitro* by a semiautomated microdilution technique. Antimicrob Agents Chemother. 1979;16(6):710-8.
16. American Diabetes Association. Diagnosis and classification of diabetes mellitus. Diabetes Care. 2009; 32(Suppl 1): S62–S67.
17. Kahn SE, Cooer ME, Prato SD. Pathophysiology and treatment of type 2 diabetes: perspectives on the past, present and future. Lancet. 2014; 383(9922):1068-83.
18. Honka MJ, Rasku Al, Bucci M, Virtanen KA, Hannukainen JC, Kalliokoski KK, et al. Insulin-stimulated glucose uptake in skeletal muscle, adipose tissue and liver: a positron emission tomography study. Eur J Endocrinol. 2018;178:523–31.
19. Collier CA, Bruce CR, Smith AC, Lopaschuk G, Dyck DJ. Metformin counters the insulin-induced suppression of fatty acid oxidation and stimulation of triacylglycerol storage in rodent skeletal muscle. Am J Physiol Endocrinol Metab. 2006;291(1):E182-9.
20. Scheen AJ. Drug interactions of clinical importance with antihyperglycaemic agents: an update. Drug Saf. 2005;28(7):601-31.
21. Fuhlendorff J, Rorsman P, Kofod H, Brand CL, Rolin B, MacKay P, et al. Stimulation of insulin release by repaglinide and glibenclamide involves both common and distinct processes. Diabetes. 1998;47(3):345-51.
22. Blicklé JF. Meglitinide analogues: a review of clinical data focused on recent trials. Diabetes Metab. 2006;32(2):113-20.

23. Yki-Järvinen H. Thiazolidinediones. N Engl J Med.2004; 351(11):1106-18.
24. Coniff RF, Shapiro JA, Seaton TB, Bray GA. Multicenter, placebo-controlled trial comparing acarbose (BAY g 5421) with placebo, tolbutamide, and tolbutamide-plus-acarbose in non-insulin-dependent diabetes mellitus. Am J Med. 1995;98(5):443-51.
25. Chiniwala N, Jabbour S. Management of diabetes mellitus in the elderly. Curr Opin Endocrinol Diabetes Obes. 2011;18(2):148-52.
26. Kawamori R, Tajima N, Iwamoto Y, Kashiwagi A, Shimamoto K, Kaku K, et al. Voglibose for prevention of type 2 diabetes mellitus: a randomized, double-blind trial in Japanese individuals with impaired glucose tolerance. Lancet. 2009;373(9675):1607-14.
27. Stonehouse AH, Darsow T, Maggs DG. Incretin-based therapies. J Diabetes 2011. (published online ahead of print).
28. Pratley RE, Salsali A. Inhibition of DPP-4: a new therapeutic approach for the treatment of type 2 diabetes. Curr Med Res Opin. 2007;23(4):919-31.
29. Barnett A. DPP-4 inhibitors and their potential role in the management of type 2 diabetes. Int J Clin Pract. 2006;60(11):1454-70.
30. Mayfield JA, White RD. Insulin therapy for type 2 diabetes: rescue, augmentation, and replacement of beta-cell function. Am Fam Physician. 2004;70(3):489-500.
31. Burge MR, Schade DS. Insulins. Endocrinol Metab Clin North Am. 1997;26(3):575-98.
32. Cameron CG, Bennett HA. Cost-effectiveness of insulin analogues for diabetes mellitus. CMAJ. 2009;180(4):400-7.
33. Manoj A, Das S, Ramachandran AK, Alex AT, Joseph A. SGLT2 inhibitors, an accomplished development in field of medical chemistry: an extensive review. Future Med Chem. 2020;10.4155/fmc-2020-0154.
34. Abdul-Ghani MA, Norton L, DeFronzo RA. Role of sodium-glucose cotransporter 2 (SGLT 2) inhibitors in the treatment of Type 2 diabetes. Endocr Rev. 2011;32(4):515-31.

35. Kanai Y, Lee WS, You G, Brown D, Hediger MA. The human kidney low affinity Na^+/glucose cotransporter SGLT2. Delineation of the major renal reabsorptive mechanism for D-glucose. J Clin Invest. 1994;93(1):397-404.

36. Wright EM. Renal Na+-glucose cotransporters. Am J Physiol Ren Physiol. 2001; 280(1):F10-F18.

37. Wright EM, Turk E. The sodium/glucose cotransport family SLC5. Pflugers Arch Eur J Physiol. 2004;447(5):510-8.

38. Vallon V. Molecular determinants of renal glucose reabsorption. Focus on "Glucose transport by human renal Na^+/D-glucose cotransporters SGLT1 and SGLT2". Am J Physiol Cell Physiol. 2011;300(1):2010-12.

39. Nauck MA. Update on developments with SGLT2 inhibitors in the management of Type 2 diabetes. Drug Des Devel Ther. 2014;8:1335-51.

40. Ehrenkranz JRL, Lewis NG, Kahn CR, Roth J. Phlorizin: a review. Diabetes Metab Res Rev. 2005;21(1):31-8.

41. Haider K, Pathak A, Rohilla A, Haider MR, Ahmad K, Yar MS. Synthetic strategy and SAR studies of C-glucoside heteroaryls as SGLT2 inhibitor: a review. Eur J Med Chem. 2019;184:111773.

42. Meng W, Ellsworth BA, Nirschl AA et al. Discovery of dapagliflozin: a potent, selective renal sodium-dependent glucose cotransporter 2 (SGLT2) inhibitor for the treatment of Type 2 diabetes. J Med Chem. 2008;51(5): 1145-9.

43. Kasahara M, Maeda M, Hayashi S, Mori Y, Abe T. A missense mutation in the Na^+/glucose cotransporter gene SGLT1 in a patient with congenital glucose-galactose malabsorption: normal trafficking but inactivation of the mutant protein. Biochim Biophys Acta Mol Basis Dis. 2001;1536(2–3): 141-7.

44. Turk E, Zabel B, Mundlos S, Dyer J, Wright EM. Glucose/galactose malabsorption caused by a defect in the Na^+/glucose cotransporter. Nature. 1991; 350(6316):354-6.

45. Katsuno K, Fujimori Y, Takemura Y et al. Sergliflozin, a novel selective inhibitor of low-affinity sodium glucose cotransporter (SGLT2). J Pharmacol Exp Ther. 2007;320(1):323-30.

46. Kumar S, Narwal S, Kumar V, Prakash O. α-glucosidase inhibitors from plants: a natural approach to treat diabetes. Pharmacogn Rev. 2011;5(9):19-29.

47. Derosa G, Maffioli P. α-Glucosidase inhibitors and their use in clinical practice. Arch Med Sci. 2012;8(5):899-906.

48. Zito SW. Insulin and drugs used to treat diabetes. In: Williams DA and Lemke TL. Foye's principal of medicinal chemistry. 7th ed. Philadelphia, Lippincott Williams and Wilkins, 2013:896.

49. Ungwitayatorn J, Wiwat C, Samee W, Nunthanavanit P, Phosrithong N. Synthesis, *in vitro* evaluation, and docking studies of novel chromone derivatives as HIV-1 protease inhibitor. J Mol Struct. 2011;1001:152-61.

BIOGRAPHY

Project teams

Project Leader/ Researcher

Name	Chirattikan Maicheen
Institutions attended	Rangsit University, 2003-2008 Bachelor of Pharmacy Mahidol University, 2008-2011: Master of Science in Pharmacy (Pharmaceutical chemistry) Mahidol University, 2014-2018: Doctor of Philosophy (Pharmaceutical chemistry and Phytochemistry)
Address	Department of Pharmaceutical Chemistry, Faculty of Pharmaceutical Sciences, Huachiew Chalermprakiet University